

Dynamical processes simulation of vibrational mounting devices and synthesis of their parameters

Abstract. A complex mathematical model of dynamic processes in vibrational mounting device for assembly robot is given. Such mathematical model makes it possible to research the starting process of the mechanism, the steady-state regimes and spatial motions of any points of the assembling part. A rational model for the motor with unbalance at controlled starting is proposed, which lead to spatial oscillations of the grab and part. With the help of ideas of the sensitivity theory the algorithm for parameters synthesis of the device by using natural modes of oscillations is developed. The following results are presented: calculations and experiments of free oscillations; synthesis of device parameters; studies of dynamic processes at the mechanism starting and at steady-state regimes, spatial motions of the characteristic points for assembling part.

Streszczenie. Podano złożony model matematyczny procesów dynamicznych w wibracyjnym urządzeniu dla robota montażowego. Taki model pozwala badać proces uruchomienia mechanizmu, tryby w stanie ustalonym i ruchy przestrzenne dowolnych punktów części złożonej. Zaproponowano model silnika z niewyważeniem przy kontrolowanym starcie, który prowadzi do przestrzennych oscylacji chwytaka i części. Za pomocą koncepcji teorii wrażliwości opracowano algorytm syntezy parametrów urządzenia za pomocą naturalnych trybów oscylacji. (Symulacja procesów dynamicznych wibracyjnych urządzeń montażowych i synteza ich parametrów).

Keywords: dynamical process, vibrational mounting device, parameters synthesis, sensitivity theory, motor, unbalance.

Słowa kluczowe: proces dynamiczny, wibracyjne urządzenie montażowe, synteza parametrów, teoria wrażliwości, silnik, niewyważenie.

Introduction

The problem of assembly automating by using of robots (manipulators) for increasing labor productivity, releasing hands, improving the work quality, as well as performing hazardous for health, physically heavy and monotonous work is actual for different industries. One of the promising directions in this problem solving is the use of uncontrolled, in particular, vibrational assembled devices. It's using allow to abandon expensive sensors and servo drives at the assembly process even for non-axisymmetric parts without chamfers, does not impose high demands on the rigidity of the entire robot design. The assembly is as follows. The robot gripper "roughly" brings the assembling part, which is installed in the grab of the vibrational assembling device, to the connection point with another part (for example, a plunger to the plunger barrel). The assembling device is turn on, the part with the grab starts to do some spatial oscillations, and the parts are mated, even though the position of the assembling part was initially inaccurate. Spatial oscillations of the grab and parts are given by an unbalanced motor, which mounted on the assembling device. In Fig. 1 shows the assembly device with a vibrational mounting mechanism.

In paper [1] mathematical models of devices for robots with low-frequency vibrations were created. Paper [2] is proposed the algorithms developments for the functioning of assembly mechanisms in shipbuilding. Paper [3] is devoted to dynamic processes simulation at starting process of vibrational mechanisms. Features of sensors and servo drive using are analyzed in paper [4], adaptive automatic grabs are considered in [5, 6]. An analysis of the design features of vibrational mounting devices is given in paper [7]. The simplest methods of parameters choosing for mechanisms are also presented there. Dynamic processes simulation in some devices with unbalanced vibro drives is devoted papers [8, 9], electromagnetic – [10, 11], mechanical – [12, 15].

The created samples of assembly devices are confirmed their high efficiency. However, the absence of mathematical models of such mechanisms, research methods, optimal choice of parameters and operating regimes makes it difficult to improve existing designs and rational

arrangement of similar devices. Researches aimed at such problems solving are very actual [24].

The research objective is the creation of a complex mathematician model of dynamical processes in the vibrational mounting device for assembly robot, the algorithm development of synthesis of their parameters. The following problems must be solved: to create a complete system of differential equations of the vibrational device; to develop the algorithm for parameters synthesis of the device by using natural modes of oscillation; to propose the rational model for the controlled starting of the unbalanced motor; to develop methods for the motion studying of mechanism links and characteristic points of mounted parts during starting and on steady-state regimes [16,17].

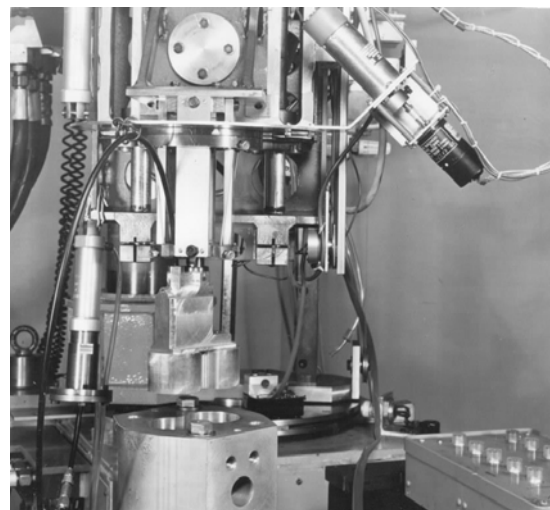


Fig.1. Assembling device with vibrational mounting mechanism

Implementation of calculation researches will be done by using of the developed model for choosing rational parameters of a particular device, dynamic processes during starting and on steady-state regimes, spatial motions of characteristic points of the mounted part [18, 19, 20].

Mathematical model of dynamical processes in vibration device

In Figure 2 the mechanism diagram for the assembly device is shown. Structurally, the device consists of several rigid bodies, connected together by elastic elements: 1 – foundation for the mechanism fixing to the "arm" of the manipulator; 2 – ring; 3 – inclined bars; 4 – grab; 5 – mounted part; 6 – plate springs; 7 – tachometre; 8 – electric motor; 9 – unbalance; 10 – plate of the elastic support of the exciter, which is bent at 45° angle and fixed to the ring so that the motor axis formed angles of 45° with directions parallel to the axes of the plate springs.

The motion equations of the mechanism can be written in the form of Lagrange's equations of the second kind.

Generalized coordinates. The fixed coordinate system is connected with the manipulator gripper, its origin is placed in the attachment plane of the grab to the plate springs (it is assumed that they are statically deformed). Axes Ox and Oy are directed along mentioned above springs, and the axis Oz – vertically upwards. The ring position in the fixed coordinate system $Oxyz$ up to infinitesimals of higher order is determined by three generalized coordinates: x , y , φ . Coordinates x and y are determined a mass centre position of the ring. The coordinate φ defines the rotation of the moving, rigidly connected coordinate system $O_1x_1y_1z_1$ relative to the fixed coordinate system.

It can be shown that the grab position relative to the ring up to infinitesimal higher orders also can be determined by three generalized coordinates: coordinates ϑ_{x_1} , ϑ_{y_1} define the grab rotation around the axes Ox_1 and Oy_1 ; coordinate $z_1 = z$ – vertical displacement of the suspension point. It have been shown by experiments that in operating regimes of the mechanism the exciter position relative to the ring is completely determined by an angular coordinate γ , and its elastic support can be modeled by a joint with a spiral spring (point O_2 in Fig. 2), the rigidity coefficient of which is easily determined experimentally [21, 22].

So the mechanism motion can be described by seven generalized coordinates: x , y , φ , ϑ_{x_1} , ϑ_{y_1} , z_1 , γ .

The total kinetic energy of the system can be written in assumption that oscillations are small in the form [3]:

$$T = m_1 \frac{\dot{x}^2 + \dot{y}^2}{2} + \frac{J_{z_1} \dot{\varphi}^2}{2} + \frac{m_2}{2} \left[(\dot{x} - l \cdot \dot{\vartheta}_{y_1})^2 + (\dot{y} + l \cdot \dot{\vartheta}_{x_1})^2 + \dot{z}_1^2 \right] - \frac{J_{\xi} \dot{\vartheta}_{x_1}^2}{2} + \frac{J_{\eta} \dot{\vartheta}_{y_1}^2}{2} + \frac{J_{\zeta} \dot{\varphi}^2}{2} + \frac{m_3}{2} \left[(\dot{x} - R_0 \dot{\varphi} \cos 45^\circ - R^* \dot{\gamma} \sin \beta \cos 45^\circ)^2 + (\dot{y} + R_0 \dot{\varphi} \cos 45^\circ - R^* \dot{\gamma} \sin \beta \cos 45^\circ)^2 + R^{*2} \dot{\gamma}^2 \cos^2 \beta \right] + \frac{J_{x'} \dot{\gamma}^2}{2} + \frac{J_{z_3} \dot{\varphi}^2}{2}$$

where m_1 – ring mass; J_{z_1} – ring inertia moment about vertical axe; m_2 – grab and part mass; l – distance from the suspension point to the mass center of the grab; J_{ξ} , J_{η} , J_{ζ} – inertia moments of the grab and the part about the principal central axes of inertia $C\xi$, $C\eta$, $C\zeta$; m_3 – exciter mass; R_0 – distance from the exciter mass to the

mechanism axis; R^* – distance from the exciter mass center to the joint axis; β – angle between the direction O_2C_1 and horizontal line; $J_{x'}$, J_{z_3} – exciter inertia moments about axes C_1x' and C_1z_3 respectively; $J_{y'}$, $J_{z'}$ – exciter inertia moments about axes C_1y' and C_1z' respectively [23].

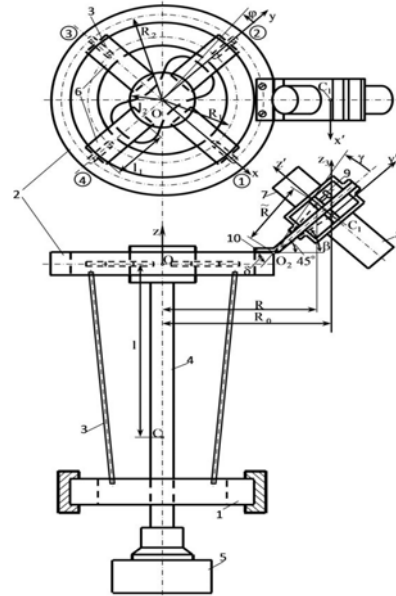


Fig. 2. Scheme of the vibrational mounting mechanism

For generalized restoring forces of small oscillations the following expressions can be written:

$$Q_x = -4cx; \quad Q_y = -4cy; \quad Q_\varphi = -4cR_0^2\varphi; \quad Q_{\vartheta_{x_1}} = -c\vartheta_{x_1}; \\ Q_{\vartheta_{y_1}} = -c\vartheta_{y_1}; \quad Q_{z_1} = -4c_1z_1; \quad Q_\gamma = -c_2\gamma,$$

where $c = \frac{12EI_{zz}}{l_c^3}$ – bar stiffness coefficient; E – steel

module of elasticity; $I_{zz} = \frac{\pi d_c^4}{64}$ – axial moment of bar cross-section (circular section); l_c – bar length; d_c – bar diameter; $c = 2a \cdot l_2 + 2d + 2d_1 + m_2 g \cdot l$; g – gravity

acceleration; $a = EI_{zz}^* \frac{12 \left(\frac{l_1}{2} + l_2 \right)}{l_1^3}$; $d = EI_{zz}^* \frac{4l_1 + 6l_2}{l_1^2}$;

$I_{zz}^* = \frac{bh^3}{12}$ – axial moment of inertia of a rectangular section of the plate spring; l_1 – free part length of the plate spring; l_2 – radius of the grab upper part; b – width of the plate spring; h – spring thickness; $d_1 = \frac{GJ_t}{l_1}$; $J_t = \alpha h^3 b$ –

resistance torque of rectangular cross-section; α – tabular coefficient dependent on the ratio h and b ; G – steel

shear module; $c_1 = \frac{12EI_{zz}^*}{l_1^3}$; c_2 – the experimental value

of the stiffness coefficient (equivalent stiffness of the elastic support of the exciter, see Fig. 2).

Perturbing forces and moments have the following form:

$$F_x = \frac{\sqrt{3}}{2} m \dot{\psi}^2 r \cos(\psi + \xi); \quad F_y = \frac{\sqrt{3}}{2} m \dot{\psi}^2 r \cos(\psi - \xi);$$

$$M_{O_1 z_1} = m \dot{\psi}^2 r R \sin \psi - I_{z'}^{(r)} \dot{\psi} \cos 45^\circ;$$

$$M_{O_2 z_4} = -m \dot{\psi}^2 r \cos \psi R \sin(\delta - 45^\circ),$$

m – unbalance mass; r – distance from the unbalance mass centre to the motor axis; $I_{z'}^{(r)}$ – total moment of inertia of the motor rotors and the tachometer about the axis z' ; R – distance from the mechanism axis to the intersection point of the motion plane of the unbalance with the motor axis; R – distance from the joint axis O_2 to the intersection point of the motor axis and motion plane of the unbalance (see Fig. 2).

In the study of steady-state regimes must be taking to account, that $\psi = \omega t$, $\dot{\psi} = \omega$, $\ddot{\psi} = 0$.

An integral effect of resistance forces is very important for considered devices, therefore, for the description simplicity, the generalized forces of resistance can be taken proportional to corresponding generalized velocities:

$$Q_x^* = -\beta_x \dot{x}, \quad Q_y^* = -\beta_y \dot{y}, \quad Q_\varphi^* = -\beta_\varphi \dot{\varphi}, \quad Q_{\vartheta_{x_1}}^* = -\beta_{\vartheta_{x_1}} \dot{\vartheta}_{x_1},$$

$$Q_{\vartheta_{y_1}}^* = -\beta_{\vartheta_{y_1}} \dot{\vartheta}_{y_1}, \quad Q_{z_1}^* = -\beta_{z_1} \dot{z}_1, \quad Q_\gamma^* = -\beta_\gamma \dot{\gamma}.$$

Inaccuracy in defining the damping coefficients β_x , β_y , β_φ , $\beta_{\vartheta_{x_1}}$, $\beta_{\vartheta_{y_1}}$, β_{z_1} , β_γ in analyzing transient regimes is not significant. It is more preferable to choose the damping coefficients by using experimental data about forced vibrations of designs prototypes at steady-state regimes, which are close to resonance.

Motion differential equation of mechanism. Let's perform a standard procedure of Lagrange equations forming of the second kind (cumbersome transformation are not shown here), the mechanism equation of motion can be written as:

$$(1) \quad \mathbf{M}\mathbf{q} + \mathbf{B}\mathbf{q} + \mathbf{C}\mathbf{q} = \mathbf{P},$$

where $\mathbf{q} = [x, y, \varphi, \vartheta_{x_1}, \vartheta_{y_1}, z_1, \gamma]^T$ – vector of generalized coordinates (τ – transpose sign); \mathbf{M} – inertia matrix;

$\mathbf{B} = \text{diag}\{\beta_x, \beta_y, \beta_\varphi, \beta_{\vartheta_{x_1}}, \beta_{\vartheta_{y_1}}, \beta_{z_1}, \beta_\gamma\}$ – diagonal damping matrix;

$\mathbf{C} = \text{diag}\{4c, 4c, 4cR^2, \tilde{c}, \tilde{c}, 4c_1, c_2\}$ – stiffness matrix;

$\mathbf{P} = [F_x, F_y, M_{O_1 z_1}, 0, 0, 0, M_{O_2 z_4}]^T$ – vector of perturbing.

Calculation and experimental researches of dynamic processes in the vibrational mounting mechanism

Frequencies and modes of the natural oscillations were experimentally determined for parameters correction of the obtained models. The lower frequency $f_1 = 5.4\text{Hz}$ corresponds to the intense rotational vibrations of the ring (other mechanism parts are practically stationary); the frequency $f_6 = 23.5\text{Hz}$ corresponds to the intensive oscillations of the grab with the part and the exciter, while the ring do less intense oscillations in the axial directions x and y , and small rotational oscillations. Modes close to the frequency 23.5Hz were the most favorable for assembly. The other frequencies were determined by oscillograms

interpretation of natural damped oscillations of the individual parts of the mechanism (ring, grab) with their various initial deflections. The following values of frequencies have been received: $f_2 = 10\text{Hz}$ (ring deflection in the axis direction x); $f_3 = 11\text{Hz}$ (ring deflection in the axis direction y); $f_4 = 16\text{Hz}$ (initial coordinate variation ϑ_{x_1} for the grab); $f_5 = 17\text{Hz}$ (initial coordinate variation ϑ_{y_1} for the grab). The frequency corresponding to a variation of the independent coordinate z_1 was not determined experimentally, since it is value much higher than the operating regimes of the mechanism.

After the problem solving of eigenvalues and eigenvectors

$$(2) \quad (-\omega^2 \mathbf{M} + \mathbf{C})\mathbf{h} = 0$$

for equation

$$(3) \quad \mathbf{M}\mathbf{q} + \mathbf{C}\mathbf{q} = 0,$$

approximate calculated values of the corresponding frequencies were obtained: $f_1 = 5.6\text{Hz}$; $f_2 = 8.36\text{Hz}$;

$f_3 = 9.24\text{Hz}$; $f_4 = 15.9\text{Hz}$; $f_5 = 18.6\text{Hz}$; $f_6 = 24.2\text{Hz}$ ($f_i = \omega_i / 2\pi$, $i = \overline{1,6}$).

Fig. 3 shows the most important modes of oscillations from a practical point of view. For better representation of oscillations modes, the angular coordinates were preliminarily multiplied by following linear dimensions: φ – on R_2 ; ϑ_{x_1} and ϑ_{y_1} – on l ; γ – on R^* . For better comparison of different oscillations modes at normalization, the coordinate ϑ_{x_1} was taken equal to unity.

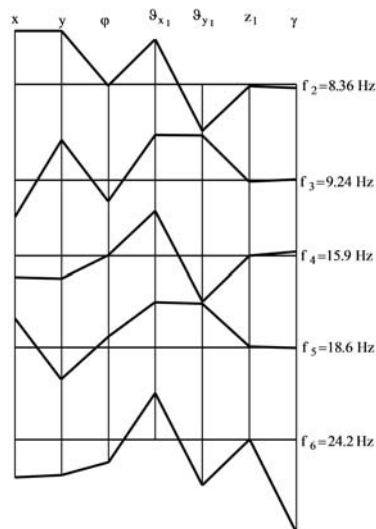


Fig. 3. Oscillations modes

Synthesis of the mechanism parameters by using natural modes of oscillations. The device feature consists in the fact that it operates near resonance. This fact makes it possible to use calculations of natural oscillations when solving an optimization problem, since the mode of natural oscillations is close to the mode of resonance oscillations. Design considerations require that at operational regime a coordinates variation ϑ_{x_1} , ϑ_{y_1} and φ was maximal (to simplify and speed up mounting), but coordinates variations x and y – were minimal (to vibrations reduce of the all mounting device). Therefore, the problem can be formulated as follows. It is needed to consider modes of natural oscillations of the mechanism model and the

favorable ones to "improve" in the sense indicated above by varying the design parameters.

A possible way of the problem solving - the use of ideas of the sensitivity theory [13, 14]. Let's assume that after solving the eigenvalues and the eigenvectors problems (2), it turns out that the eigenvector \mathbf{h}_i ($i = \overline{1, n}$; in our case $n = 7$) get a more favorable form of \mathbf{h}_i^* . Denote the change \mathbf{h}_i by

$$(4) \Delta \mathbf{h}_i = \mathbf{h}_i^* - \mathbf{h}_i.$$

Assuming that $\Delta \mathbf{h}_i$ is sufficiently small, let's introduce the partial derivatives of the vector \mathbf{h}_i with respect to the variable parameters p_k ($k = \overline{1, m}$), then, up to second-order infinitesimal, it can be written

$$(5) \Delta \mathbf{h}_i = \sum_{k=1}^m \frac{\partial \mathbf{h}_i}{\partial p_k} \Delta p_k,$$

where Δp_k - change of the k -th parameter. It is obvious, that the following decomposition can be presented as

$$(6) \frac{\partial \mathbf{h}_i}{\partial p_k} = \sum_{j=1}^n a_{ijk} \mathbf{h}_j \quad (j = \overline{1, n}).$$

If now expression $(-\omega_i^2 \mathbf{M} + \mathbf{C}) \mathbf{h}_i = 0$ differentiate with respect to the parameter p_k and multiply the resulting expression from left side by \mathbf{h}_i^T ($l \neq i$), then taking into account (6) can be obtained

$$(7) a_{ilk} = \frac{\mathbf{h}_l^T \left(\frac{\partial \mathbf{C}_k}{\partial p_k} - \omega_i^2 \frac{\partial \mathbf{M}_k}{\partial p_k} \right) \mathbf{h}_i}{(\omega_l^2 - \omega_i^2) \mathbf{h}_l^T \mathbf{M} \mathbf{h}_i}.$$

If $l = i$, it makes sense to assume $a_{iik} = 0$. With taking into account (6) the expression (5) can be written as

$$(8) \Delta \mathbf{h}_i = \mathbf{S} \Delta \mathbf{p},$$

$$\text{where } \mathbf{S} = \begin{bmatrix} \sum_{j=1}^n a_{ij1} \mathbf{h}_{1j} & \cdots & \sum_{j=1}^n a_{ijm} \mathbf{h}_{1j} \\ \vdots & \ddots & \vdots \\ \sum_{j=1}^n a_{ij1} \mathbf{h}_{nj} & \cdots & \sum_{j=1}^n a_{ijm} \mathbf{h}_{nj} \end{bmatrix} \quad \text{-- sensitivity matrix;}$$

$\Delta \mathbf{p} = [\Delta p_1, \dots, \Delta p_m]^T$ - vector of parameters variation.

Expression (8) can be considered as an equation in $\Delta \mathbf{p}$. Depending from ratio of n and m for $\Delta \mathbf{p}$, we have the following:

$$(9) \Delta \mathbf{p} = (\mathbf{S}^T \mathbf{S})^{-1} \mathbf{S}^T \Delta \mathbf{h}_i \quad (m < n);$$

$$(10) \Delta \mathbf{p} = \mathbf{S}^{-1} \Delta \mathbf{h}_i \quad (m = n);$$

$$(11) \Delta \mathbf{p} = \mathbf{S}^T (\mathbf{S} \mathbf{S}^T)^{-1} \Delta \mathbf{h}_i \quad (m > n).$$

The formula (9) is obtained by the least-squares method. With the help of expression (11), from an infinite set of solutions, the only one that has a property $\|\Delta \mathbf{p}\|_2 \rightarrow \min$.

The new value of parameter vector, which is corresponding to the changed form, can be approximately represented as the following equation:

$$(12) \mathbf{p} = \mathbf{p}_0 + \Delta \mathbf{p}$$

where \mathbf{p}_0 - initial parameter vector.

In formula (5) $\Delta \mathbf{h}_i$ is assumed small, which is rarely can be done. For large values of $\Delta \mathbf{h}_i$, it is needed to develop a special algorithm, that allows one to determine the necessary parameters variations by using one of the formulas (9)-(11). If the modules of some coordinates in the vector $\Delta \mathbf{h}_i$ are large, then the first step is executed with

$$\Delta \mathbf{h}_i = \frac{\tilde{\Delta \mathbf{h}_i}}{r} \quad (r = 1, 2, \dots); \quad r \text{ is chosen so that the module}$$

Δh_{ji} ($j = \overline{1, n}$) is small, for example, less than 5% of the

module h_{ji} . At every step an iterative process is realized. After the first iteration by using formula (9) can be obtained a parameter vector $\mathbf{p}^{(1)}$ and a new eigenvector $\mathbf{h}_i^{(1)}$. In a

general case the last one differs from the vector $\mathbf{h}_i + \Delta \mathbf{h}_i$, i.e. vector, which we try to attain on the first step. Further the residual $\Delta \mathbf{h}_i^{(1)} = \mathbf{h}_i + \Delta \mathbf{h}_i - \mathbf{h}_i^{(1)}$ can be determined and can be executed a second iteration with it to find $\mathbf{p}^{(2)}$,

$\mathbf{h}_i^{(2)}$. Then the residual can be calculated

$\Delta \mathbf{h}_i^{(2)} = \mathbf{h}_i + \Delta \mathbf{h}_i - \mathbf{h}_i^{(2)}$. The iterative process continues until the fulfillment of the condition will be done

$$\frac{|p_k^{(j+1)} - p_k^{(j)}|}{|p_k^{(j)}|} < \varepsilon \quad (k = \overline{1, m}),$$

where ε - some small number.

The eigenvector $\mathbf{h}_i^{(j+1)}$ obtained at the last iteration is taken as the vector \mathbf{h}_i , with its help we refine $\Delta \mathbf{h}_i$ by using formula (4) and execute the second step with the

$\Delta \mathbf{h}_i = \frac{\tilde{\Delta \mathbf{h}_i}}{r-1}$ same as the first. The last r -th step is obviously executed for

$$\Delta \mathbf{h}_i = \frac{\tilde{\Delta \mathbf{h}_i}}{r - (r-1)} = \tilde{\Delta \mathbf{h}_i}.$$

We note an important fact in the software implementation of the algorithm. The initial improved vector form \mathbf{h}_i^* , as well as the improved forms at each algorithm step should be normalized, and the normalization should be the same as in the subroutine for determining of eigenvalues and eigenvectors.

It is noted that such method can be used in the case of simultaneous correction of several modes of oscillations by using of block matrices.

Optimization results by using modes of oscillations.

Calculation researches of the mechanism have been done by using the following parameters:

$$m_1 = 0.607 \text{ kg}; \quad m_2 = 0.534 \text{ kg}; \quad m_3 = 0.502 \text{ kg};$$

$$J_{z_1} = 0.517 \cdot 10^{-3} \text{ kg} \cdot \text{m}^2; \quad J_{x_1} = 0.2019 \cdot 10^{-2} \text{ kg} \cdot \text{m}^2;$$

$$J_{y_1} = 0.1873 \cdot 10^{-2} \text{ kg} \cdot \text{m}^2; \quad J_{z_2} = 0.600 \cdot 10^{-4} \text{ kg} \cdot \text{m}^2;$$

$$J_{x'} = 0.6715 \cdot 10^{-2} \text{ kg} \cdot \text{m}^2; \quad J_{y'} = 0.6715 \cdot 10^{-2} \text{ kg} \cdot \text{m}^2;$$

$J_{z'} = 0.642 \cdot 10^{-4} \text{ kg} \cdot \text{m}^2$; $R_0 = 0.15 \text{ m}$; $R^* = 0.05 \text{ m}$;
 $l = 0.17 \text{ m}$; $l_c = 0.088 \text{ m}$; $d_c = 0.002 \text{ m}$; $R_2 = 0.048 \text{ m}$;
 $b = 0.01 \text{ m}$; $h = 0.0014 \text{ m}$; $l_1 = 0.025 \text{ m}$; $l_2 = 0.015 \text{ m}$;
 $\beta = 45^\circ$; $c_2 = 0.1747 \cdot 10^3 \text{ N} \cdot \text{m}$; $E = 0.21 \cdot 10^6 \text{ MPa}$;
 $G = 0.8 \cdot 10^5 \text{ MPa}$; $\alpha = 0.3$ (corresponds to $b/h \approx 7$).

As variable parameters, were considered: $p_1 = d_c^4$; $p_2 = h^3$. Such parameters are not included in the inertia matrix, therefore $\frac{\partial \mathbf{M}}{\partial p_1} = \frac{\partial \mathbf{M}}{\partial p_2} = 0$. For derivatives of the stiffness

matrix have the following expressions:

$$\frac{\partial \mathbf{K}}{\partial p_1} = \text{diag} \left\{ 4 \frac{3\pi E}{16l_c^3}, 4 \frac{3\pi E}{16l_c^3}, 4R_2^2 \frac{3\pi E}{16l_c^3}, 0, 0, 0, 0 \right\};$$

$$\frac{\partial \mathbf{K}}{\partial p_2} = \text{diag} \left\{ 0, 0, 0, s \cdot b \cdot s \cdot b, 4 \frac{Eb}{l_1^3}, 0 \right\},$$

$$\text{where } s = \frac{l_2(l_1 + 2l_2)E}{l_1^3} + \frac{(4l_1 + 6l_2)E}{6l_1^2} + \frac{0,6G}{l_1}.$$

Fig. 4 shows optimization results of the fifth mode of. As the preferable mode of oscillation, a calculated mode was chosen, in which the value of the coordinate φ was increased by 30% and the coordinates values x and y were decreased by the same percentage; values of others coordinates were taken without changes.

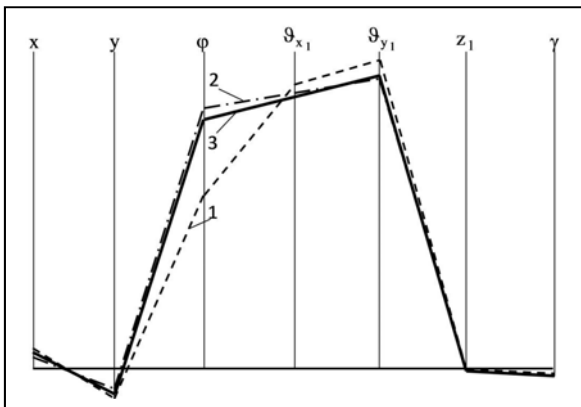


Fig. 4. Optimization of the fifth mode of oscillations: 1 – initial; 2 – preferable; 3 – after optimization

In the figure, this mode is shown after the corresponding normalization used in the program $h_5 h_5^T = 1$, because of what the coordinates values ϑ_{x_1} , ϑ_{y_1} and γ have smaller values than the original mode. Modes of oscillations are presented here without additional normalization, which was mentioned above. It can be seen from the figure that the obtained mode after optimization has a more preferable form than the original one, especially for the coordinate φ . The values of the variable parameters were recognized as follows: $d_c = 0.288 \cdot 10^{-2} \text{ m}$; $h = 0.177 \cdot 10^{-2} \text{ m}$. Corresponding value of the fifth frequency was equal to 24.25 Hz. This value is close to a slightly increased value of the sixth frequency, so the further program execution was terminated, since a small increase in the parameters would lead to a change in the number of the optimized mode. Such fact must be taken into account in the program.

Studies of steady-state and transient regimes.

The created full model (1) allows to analyze the dynamic processes of both the mechanism starting process, and the steady-state regimes, to study a geometry of movements of the device links and the mounted parts. It is needed for a complete problems solution of synthesis parameters of the device.

At components forming of the perturbation vector, it was assumed that the dependence of the angular speed of the motor rotor on the time has the form shown in the graph of Fig. 5. Such dependence is shown for the time moment of the device actuation.

For the time interval $0 \leq t \leq t_0$, the quadratic law of angular speed variation is taken, which well consistent with the experimental data. The dependence of the rotation angle from the motor rotor on the time can be presented as:

$$\psi = \begin{cases} -\frac{\omega_0(t-t_0)^3}{3t_0^2} + \omega_0 t - \frac{\omega_0 t^3}{3}, & t \leq t_0; \\ \frac{2}{3}\omega_0 t_0 + \omega_0(t-t_0), & t > t_0, \end{cases}$$

where ω_0 – angular speed of the steady-state regime (controlled parameter); t_0 – transient time.

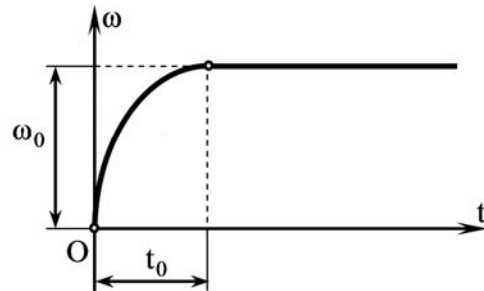


Fig. 5. Law of variation in the motor angular speed at starting

The law of variation in the generalized coordinates x , y , φ , ϑ_{x_1} at the device starting is illustrated in Fig. 6-9.

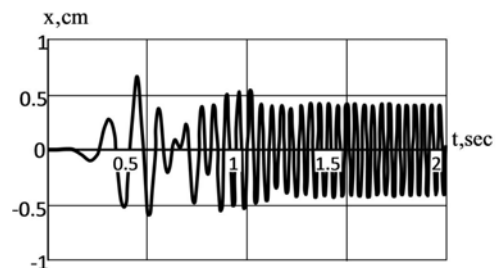


Fig. 6. Law of variation in the coordinate x

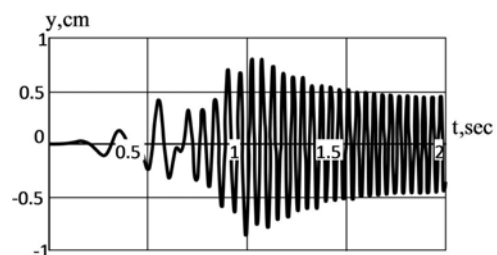


Fig. 7. Law of variation in the coordinate y

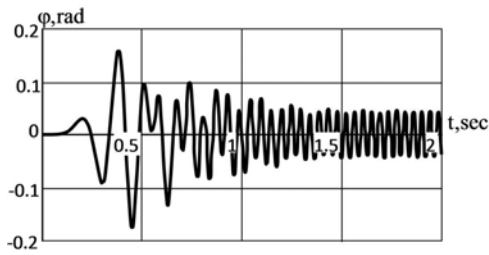


Fig. 8. Law of variation in the rotation angle φ

Calculations have been done at $t_0 = 2\text{sec}$, $\omega_0 = 152.05\text{rad/sec}$ ($n_0 = 1452\text{prn}$). In this case resonance oscillations are realized near the fifth natural frequency of the mechanism ($\nu_5 = 24.2\text{Hz}$), when the coordinates vary significantly ϑ_{x_1} , ϑ_{y_1} and sufficiently significant varies in the coordinates x , y , φ . Such regime leads to a quick parts mating, which is consistent with the experiments.

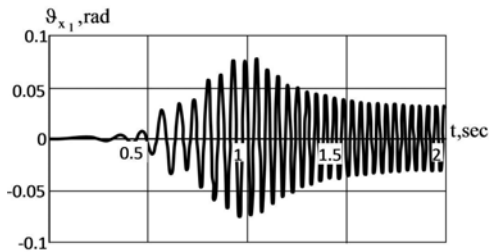


Fig. 9. Law of variation in the rotation angle ϑ_{x_1}

The spatial motions of some characteristic points of the foundation of the mounted part (Fig. 10; the coordinates are given in millimeters) are shown in Fig. 11-13.

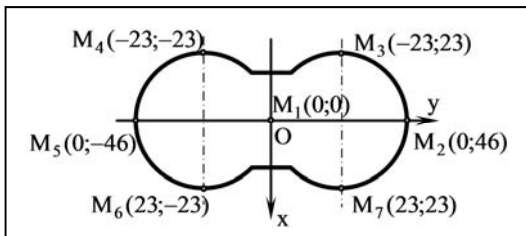


Fig. 10. Location of characteristic points of the foundation of the mounted part

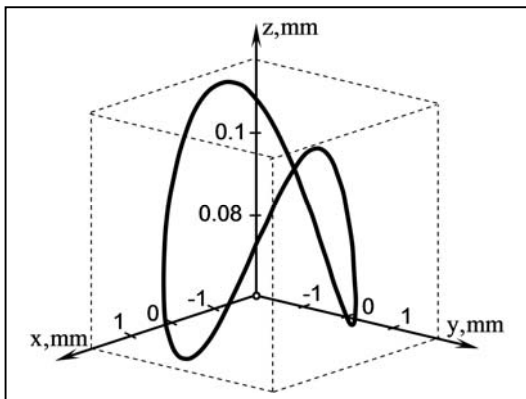


Fig. 11. Trajectory of point motion M_1

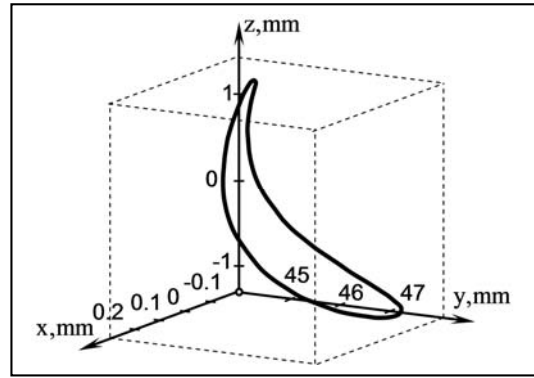


Fig. 12. Trajectory of point motion M_2

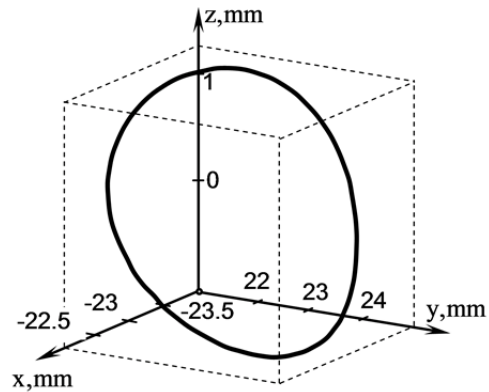


Fig. 13. Trajectory of point motion M_3

Conclusions

1. A complex mathematical model of dynamic processes in vibrational mounting device for assembly robot is created. Such mathematical model makes it possible to research the starting process of the mechanism, the steady-state regimes and spatial motions of any points of the assembling part.
2. A rational model for the motor with unbalance at controlled starting is proposed, which lead to spatial oscillations of the grab and part.
3. With a help of ideas of the sensitivity theory the algorithm for parameters synthesis of the device by using natural modes of oscillations is developed.
4. Calculation and experimental researches of free oscillations of the particular device for the parameters correction have been done.
5. The results of the parameters synthesis of the device for mounting a particular part are presented.
6. The results of calculation researches of the dynamic processes during starting and on steady-state regimes of the mechanism at the part mounting are given.
7. The spatial motions of the characteristic points of the mounted part have been researched.
8. The research results are perspective in simulation and improvement of a similar designs.

Authors: Dr. Techn. Sc., Prof., Vladimir M. Shatokhin, Head of the Department of Theoretical Mechanics, Kharkiv National University of Civil Engineering and Architecture, 40 Sumska Str., Kharkiv, 61002, Ukraine, e-mail: shatokhinvlm@gmail.com; PhD. Techn. Sc., Ass. Prof., Vladimir M. Sobol, Department of Theoretical Mechanics, Kharkiv National University of Civil Engineering and Architecture, 40 Sumska Str., Kharkiv, 61002, Ukraine, e-mail: sobol_vn@ukr.net; Prof. Waldemar Wójcik, Lublin University of Technology, Institute of Electronics and Information Technology, Nadbystrzycka 38A, 20-618 Lublin, Poland, e-mail: waldemar.wojcik@pollub.pl; M.Sc. Aisha Mussabekova, Kazakh

REFERENCES

- [1] Vartanov, M.V., Bojkova, L.V., Zinina, I.N., Mathematical model of robotic assembly by means of adaptation and low-frequency vibration, *Assembly Automation*, 37 (2017), 130-134.
- [2] Qu, S., Jiang, Z., A memetic algorithm approach for batch-model assembly line balancing problem of sub-block in shipbuilding, Proceedings of the Institution of Mechanical Engineers Part B, *Journal of Engineering Manufacture*, 228 (10) (2014), 1290-1304.
- [3] Shatokhin, V.M., Dynamical processes simulation in vibrational mounting devices for assembly robots, *Vibrations in technique and technology*, 3 (59) (2010), 143-153.
- [4] Felip, J., Morales, A., Robust sensor-based grasp primitive for a three-finger robot hand, In: IEEE/RSJ International Conference on Intelligent Robots and Systems (2009), 1811–1816.
- [5] Gomez, G., Hernandez, A., Hotz, P.E., An adaptive neural controller for a tendon driven robotic hand, In: 9th International Conference on Intelligent Autonomous Systems (IAS-9) (2006), 298–307.
- [6] Miller, A.T., Knoop, S., Christensen, H.I., Allen, P.K., Automatic grasp planning using shape primitives, In: IEEE International Conference on Robotics and Automation 2 (2003), 1824–1829.
- [7] Jcobi, P., Fügemechnismen für die automatisierte Montage mit Industrierobotern, *Karl-Marx-Stadt, Wissenschaftliche Zeitschrift der Technischen Hochschule*, (1982), 96.
- [8] Shatokhin, V.M., About the identification of parameters of unbalanced oscillating devices with eccentric rotor and asynchronous drive, *Vibrations in technique and technology*, 3 (83) (2017), 41-50.
- [9] iselovskaya, E.V., Panovko, G.Ya., Shokhin, A.E., Oscillations of the mechanical system, excited by unbalanced rotor of induction motor. *Journal of Machinery Manufacture and Reliability*, 42 (6) (2013), 457–462.
- [10] Gorbatiyk, R., Palamarchuk, I., Chubuk, R., Electromechanical model of machine for vibroabrasive treatment of machine parts. *Ukrainian journal of mechanical engineering and materials science*, 1 (1) (2015), 35–44.
- [11] Cherno, A.A., Control of resonant electromagnetic vibration drive using a digital filtering algorithm based on discrete Fourier transform. *Journal of automation and information sciences*, 46 (2014), 53-68.
- [12] Ragulskis, K., Some problems of nonlinear precise vibromechanics and vibroengineering (summary). *Journal of vibroengineering*, 13 (2011), n.3, 590-618.
- [13] Akhtar, I., Borggaard, J., Hay, A., Shape sensitivity analysis in flow models using a finite-difference approach. *Mathematical problems in engineering*, 2010 (2010), ID 209780, 22.
- [14] White, Ch.,W., Maytum, B.D., Eigensolution sensitivity to parametric model perturbations. *The shock and vibration bulletin*, 46 (1996), 123–133.
- [15] Vasilevskiy, O.M. Metrological characteristics of the torque measurement of electric motors, *International Journal of Metrology and Quality Engineering*, 8, art. no. 7, (2017). DOI: 10.1051/ijmqe/2017005
- [16] Vasilevskiy, O.M., Kulakov, P.I., Ovchynnykov, K.V., Didych, V.M. Evaluation of dynamic measurement uncertainty in the time domain in the application to high speed rotating machinery, *International Journal of Metrology and Quality Engineering*, 8, art. no. 25, (2017). DOI: 10.1051/ijmqe/2017019
- [17] Vasilevskiy, O.M. Methods of determining the recalibration interval measurement tools based on the concept of uncertainty, *Technical Electrodynamics* 6 (2014), 81-88.
- [18] Vedmitskiy, Y.G., Kukharchuk, V.V., Hraniak, V.F. New non-system physical quantities for vibration monitoring of transient processes at hydropower facilities, integral vibratory accelerations // *Przeglad Elektrotechniczny* 93 (3) (2017), 69-72.
- [19] Kukharchuk, V.V., Kazyv, S.S., Bykovsky, S.A., Discrete wavelet transformation in spectral analysis of vibration processes at hydropower units, *Przeglad Elektrotechniczny* 93 (5) (2017), 65-68.
- [20] Kukharchuk V.V., Hraniak V.F., Vedmitskiy Y.G., Bogachuk V.V., and etc. "Noncontact method of temperature measurement based on the phenomenon of the luminophor temperature decreasing", Proc. SPIE 10031, *Photonics Applications in Astronomy, Communications, Industry, and High-Energy Physics Experiments 2016*, 100312F (28 September 2016).
- [21] Kukharchuk V.V., Bogachuk V.V., Hraniak V.F., Wójcik W., Suleimenov B., Karnakova G., "Method of magneto-elastic control of mechanic rigidity in assemblies of hydropower units", Proc. SPIE 10445, *Photonics Applications in Astronomy, Communications, Industry, and High Energy Physics Experiments 2017*, 104456A (7 August 2017).
- [22] Azarov O.A., Dudnyk O.V., Kaduk O.V., Smolarz A., Burlibay A., "Method of correcting of the tracking ADC with weight redundancy conversion characteristic", Proc. SPIE 9816, *Optical Fibers and Their Applications 2015*, 98161V (17 December 2015).
- [23] Osadchuk V.S., Osadchuk A.V. The magneticreactive effect in transistors for construction transducers of magnetic field, *Electronics and Electrical Engineering*. – Kaunas: Technologija, 3 (109) (2011), 119-122.
- [24] Ostrowski M., Jarzyna W., Vibration reduction of nonlinear object with an adaptive proportional-derivative controller with a mras structure. *Informatyka Automatyka Pomiarowy w Gospodarce I Ochronie Środowiska IAPGOŚ* 6(1)/2016, 51–54.